

Improving interferometers by quantum light: toward testing
quantum gravity on an optical bench

Original

Improving interferometers by quantum light: toward testing
quantum gravity on an optical bench / Ivano Ruo, Berchera; Ivo P., Degiovanni; Stefano, Olivares; Paolo, Traina;
Samantaray, NIGAM LAHARI; M., Genovese. - In: Improving interferometers by quantum light: toward testing quantum
gravity on an optical bench. - 9980:99800F(2016), pp. 1-9. [10.1117/12.2235413]

Availability:

This version is available at: 11583/2664626 since: 2017-02-02T15:00:31Z

Publisher:

Proc. of SPIE

Published

DOI:10.1117/12.2235413

Terms of use:

This article is made available under terms and conditions as specified in the corresponding bibliographic description in
the repository

Publisher copyright

(Article begins on next page)

Improving interferometers by quantum light: toward testing quantum gravity on an optical bench

Ivano Ruo-Berchera^a, Ivo P. Degiovanni^a, Stefano Olivares^{c,e}, Paolo Traina^a, Nigam Samantaray^{a,b}, and M. Genovese^{a,d}

^aINRIM-Istituto Nazionale di Ricerca Metrologica, Torino I-10135, Italy

^bPolitecnico di Torino, Corso Duca degli Abruzzi, 24 - I-10129 Torino, Italy

^cDipartimento di Fisica, Università degli Studi di Milano, Via Celoria 16, I-20133 Milano, Italy

^dINFN, Sezione di Torino, Via P. Giuria 1, I-10125 Torino, Italy

^eINFN, Sezione di Milano, Via Celoria 16, I-20133 Milano, Italy

ABSTRACT

We analyze in detail a system of two interferometers aimed at the detection of extremely faint phase fluctuations. The idea behind is that a correlated phase-signal like the one predicted by some phenomenological theory of Quantum Gravity (QG) could emerge by correlating the output ports of the interferometers, even when in the single interferometer it confounds with the background. We demonstrated that injecting quantum light in the free ports of the interferometers can reduce the photon noise of the system beyond the shot-noise, enhancing the resolution in the phase-correlation estimation. Our results confirms the benefit of using squeezed beams together with strong coherent beams in interferometry, even in this correlated case. On the other hand, our results concerning the possible use of photon number entanglement in twin beam state pave the way to interesting and probably unexplored areas of application of bipartite entanglement and, in particular, the possibility of reaching surprising uncertainty reduction exploiting new interferometric configurations, as in the case of the system described here.

Keywords: Quantum Optics, Quantum Metrology, Non-Classical correlation, Entanglement, Quantum Gravity Tests

1. INTRODUCTION

The dream of building a theory of unifying general relativity and quantum mechanics has been a key element in theoretical physics research for the last 60 years. Despite several proposed theories no testable prediction emerged from these studies, leading to the common belief that this research activity is more properly a part of mathematics than of physics. In the last few years the common wisdom that these theories are unable to produce experimentally testable predictions has been challenged.¹⁻⁵ In particular, more recently, effects in interferometers connected to non-commutativity of position variables⁶ in different directions have been considered both for cavities with microresonators³ and two coupled interferometers,⁵ the so called "holometer". In particular this last idea led to the construction of a double 40 meter interferometer at Fermilab.⁷ The idea at the basis of the holometer is that non-commutativity at the Planck scale ($l_p = 1.61610^{-35}$ m) of position variables in different directions leads to an additional phase noise, referred to as holographic noise (HN). In a single interferometer this noise substantially confounds with other sources of noise, even though the most sensible gravitational wave interferometers are considered, since their HN resolution is worse than their resolution to gravitational-wave at low frequencies. Nonetheless, if the two equal interferometers of the holometer are in the same spacetime volume (in particular when their arms are nearly overlapping) then the HN between them is correlated and easier to be identified.⁵ Indeed, the ultimate limit for holometer sensibility, as for any classical-light based apparatus, is dictated by the shot noise: therefore, the possibility of going beyond this limit by exploiting quantum optical states is of the greatest interest in this emergent research of exotic quantum gravity effects

Further author information: (Send correspondence to I.Ruo-Berchera)
I.Ruo-Berchera.: E-mail: i.ruoberchera@inrim.it

in the low-energy regimes. The possibility of exceeding shot-noise limit in gravitational-wave detectors have been already demonstrated⁸ by using squeezed light. In this talk it is shown that this resource can indeed allow an improvement of holometer-like apparatuses as well.^{9,10} Nonetheless, in this case, having two coupled interferometers, the full exploitation of properties of quantum light, and in particular of entanglement, lead to much larger improvements if high efficiency can be reached. We demonstrated the existence of two regimes: one, experimentally more affordable, in which injecting in the two interferometers either entangled twin beam or a pair of independent squeezed beams gives similar enhancement and a second one, more challenging, in which twin beam outperforms the double squeezing.¹⁰

In Sec. 2, we introduce the double interferometric scheme the properties of the HN. In Sec. 3, we discuss the theoretical model for the description of the HN correlation measurement and the approximations used. We also introduce the two quantum strategies for the uncertainty reduction, the one exploiting independent squeezed beam and the one which take advantage of the bipartite quantum correlations. In Sec. 4, results are presented and largely discussed. In particular the origin of the two different regimes concerning the TWB performance are pointed out as well as the role of the photon number entanglement. Conclusion are drawn in Sec. 5

2. THE DOUBLE INTERFEROMETRIC SCHEME

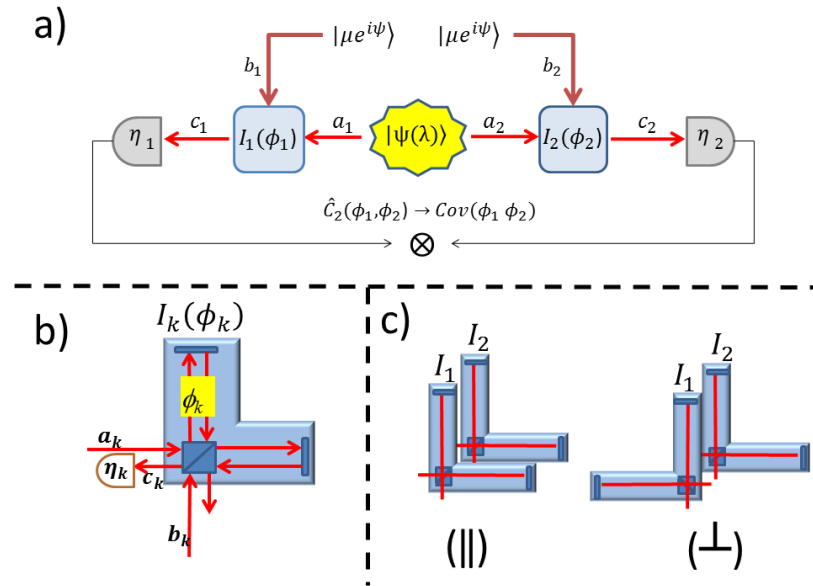


Figure 1. a) Double interferometer scheme. The modes of the bipartite input state $|\Psi(\lambda)\rangle$ are mixed with two identical coherent states $|\sqrt{\mu}e^{i\psi}\rangle$ in two interferometers $\mathcal{I}_1(\phi_1)$ and $\mathcal{I}_2(\phi_2)$. A joint detection is performed and the observable $\hat{C}(\phi_1, \phi_2)$ is measured. b) Scheme of the single Michelson interferometer $\mathcal{I}_k(\phi_k)$, where ϕ_k is the relative phase shift between the two arms. c) The two measurement configurations of the holometer suggested in order to reveal the holographic noise (HN). In the \parallel configuration the arms of the two interferometers are parallel and they share the same light cone, while in the \perp configuration one of the two interferometers is rotated by 90 degrees. See the text for further details.

Let us consider a system as depicted in Fig. 1a. Two interferometers \mathcal{I}_k ($k = 1, 2$, see the detail in Fig. 1b) are injected at the ports denoted by the mode annihilation operators b_k by a couple of identical coherent beams $|\sqrt{\mu}e^{i\psi}\rangle_{b_k}$, while the remaining ports identified by the mode operator a_k (unused in the classical scheme) are fed with a quantum state $|\Psi(\lambda)\rangle_{a_1, a_2}$, where λ is the mean number of photon in each mode. The readout ports are denoted by the mode operator c_k which will be function of the phases shifts ϕ_k among the arm of each interferometer, $c_k = c_k(\phi_k)$. Therefore, a final combination of the outputs results in an observable $\hat{C}(c_1, c_2, h.c.) = \hat{C}(\phi_1, \phi_2)$. A proper choice of the operator \hat{C} leads to an estimation of the phase-noise correlation. Here, it is useful to recall the properties that the input-output operator relations of a linear interferometer

(for example a Michelson-type) are equivalent to the ones of a beam splitter (BS) with transmission coefficient $\tau = \cos^2(\phi/2)$. In the rest of the paper we will refer to τ as the *interferometer transmission*.

The losses in the system are taken into account by considering in both channels two identical detectors with the same quantum efficiency, $\eta_1 = \eta_2 = \eta$.

In order to reveal the HN, the holometer exploits two different configurations (Fig. 1c): the one, “ \parallel ”, where HN phase fluctuation is expected to be correlated between the two interferometers, since they share the same space time volume, and the other, “ \perp ”, where HN should be causally independent (see Ref⁵). The statistical properties of the phase-shift (PS) fluctuations due to the HN may be described by the joint probability density functions $f_{\parallel}(\phi_1, \phi_2)$ and $f_{\perp}(\phi_1, \phi_2)$. We make two reasonable hypotheses about $f_x(\phi_1, \phi_2)$, $x = \parallel, \perp$. First, the marginals $\mathcal{F}_x^{(k)}(\phi_k) = \int d\phi_h f_x(\phi_k, \phi_h)$, $h, k = 1, 2$ with $k \neq h$, are exactly the same in the two configurations, i.e. $\mathcal{F}_{\parallel}^{(k)}(\phi_k) = \mathcal{F}_{\perp}^{(k)}(\phi_k)$: one cannot distinguish between the two configurations just by addressing one interferometer. Second, only in configuration “ \perp ” it is $f_{\perp}(\phi_1, \phi_2) = \mathcal{F}_{\perp}^{(1)}(\phi_1)\mathcal{F}_{\perp}^{(2)}(\phi_2)$, i.e., there is no correlation between the PSs due to the HN.⁹

A further assumption is that the characteristic measurement time is much longer than the typical time scale of the HN fluctuations as well as of the coherence time of the light. Thus, we introduce the double average \mathcal{E}_x of the measurement operator $\hat{C}(\phi_1, \phi_2)$, both over the quantum state $\langle \hat{C}(\phi_1, \phi_2) \rangle$ and over f_x ,

$$\mathcal{E}_x [\hat{C}(\phi_1, \phi_2)] \equiv \int \langle \hat{C}(\phi_1, \phi_2) \rangle f_x(\phi_1, \phi_2) d\phi_1 d\phi_2 \quad (1)$$

3. PHASE COVARIANCE ESTIMATION

The phase fluctuations due to the HN are expected to be extremely small. Therefore one is allowed to expand $\hat{C}(\phi_1, \phi_2)$ around the central values of the phase $\phi_{k,0}$ of the interferometer \mathcal{I}_k ($k = 1, 2$), i.e.

$$\hat{C}(\phi_1, \phi_2) \approx \hat{C}(\phi_{1,0}, \phi_{2,0}) + \sum_k \partial_{\phi_k} \hat{C}(\phi_{1,0}, \phi_{2,0}) \delta\phi_k + \frac{1}{2} \sum_k \partial_{\phi_k, \phi_k}^2 \hat{C}(\phi_{1,0}, \phi_{2,0}) \delta\phi_k^2 + \partial_{\phi_1, \phi_2}^2 \hat{C}(\phi_{1,0}, \phi_{2,0}) \delta\phi_1 \delta\phi_2 \quad (2)$$

where $\delta\phi_k = \phi_k - \phi_{k,0}$, and $\partial_{\phi_1^h, \phi_2^k}^{h+k} \hat{C}(\phi_{1,0}, \phi_{2,0})$ is the $(h+k)$ -th order derivative of $\hat{C}(\phi_1, \phi_2)$ calculated at $\phi_k = \phi_{k,0}$.

In turn, by evaluating the mean value of of Eq. (2) both on the quantum state and on the HN distribution (see Eq. 1), we have:

$$\mathcal{E}_x [\hat{C}(\phi_1, \phi_2)] \approx \langle \hat{C}(\phi_{1,0}, \phi_{2,0}) \rangle + \frac{1}{2} \sum_i \langle \partial_{\phi_i, \phi_i}^2 \hat{C}(\phi_{1,0}, \phi_{2,0}) \rangle \mathcal{E}_x [\delta\phi_i^2] + \langle \partial_{\phi_1, \phi_2}^2 \hat{C}(\phi_{1,0}, \phi_{2,0}) \rangle \mathcal{E}_x [\delta\phi_1 \delta\phi_2] \quad (3)$$

where we used $\mathcal{E}_x [\delta\phi_k] = 0$. Then, according to the assumptions on $f_x(\phi_1, \phi_2)$ we have $\mathcal{E}_{\parallel} [\delta\phi_k^2] = \mathcal{E}_{\perp} [\delta\phi_k^2]$ and $\mathcal{E}_{\perp} [\delta\phi_1 \delta\phi_2] = \mathcal{E}_{\perp} [\delta\phi_1] \mathcal{E}_{\perp} [\delta\phi_2] = 0$, and from Eq. (3) follows that the phase-covariance may be written as:

$$\mathcal{E}_{\parallel} [\delta\phi_1 \delta\phi_2] \approx \frac{\mathcal{E}_{\parallel} [\hat{C}(\phi_1, \phi_2)] - \mathcal{E}_{\perp} [\hat{C}(\phi_1, \phi_2)]}{\langle \partial_{\phi_1, \phi_2}^2 \hat{C}(\phi_{1,0}, \phi_{2,0}) \rangle}, \quad (4)$$

that is proportional to the difference between the mean values of the operator $\hat{C}(\phi_1, \phi_2)$ as measured in the two configurations “ \parallel ” and “ \perp ”.

Now, one has to reduce as much as possible the uncertainty associated with its measurement namely (we still assume $\delta\phi_1, \delta\phi_2 \ll 1$):

$$\mathcal{U}(\delta\phi_1 \delta\phi_2) \approx \frac{\sqrt{\text{Var}_{\parallel} [\hat{C}(\phi_1, \phi_2)] + \text{Var}_{\perp} [\hat{C}(\phi_1, \phi_2)]}}{\left| \langle \partial_{\phi_1, \phi_2}^2 \hat{C}(\phi_{1,0}, \phi_{2,0}) \rangle \right|}, \quad (5)$$

where $\text{Var}_x [\hat{C}(\phi_1, \phi_2)] \equiv \mathcal{E}_x [\hat{C}^2(\phi_1, \phi_2)] - \mathcal{E}_x [\hat{C}(\phi_1, \phi_2)]^2$.

Under the same hypotheses used for deriving Eq. (4) we can calculate the variance of $\hat{C}(\phi_1, \phi_2)$ as

$$\text{Var}_x [\hat{C}(\phi_1, \phi_2)] \approx \text{Var} [\hat{C}(\phi_{1,0}, \phi_{2,0})] + \Sigma_k A_{kk} \mathcal{E}_x [\delta\phi_k^2] + A_{12} \mathcal{E}_x [\delta\phi_1 \delta\phi_2] \quad (6)$$

where the coefficients A_{kj} ($k, j = 1, 2$) are combinations of derivative of the operator $\hat{C}(\phi_1, \phi_2)$ evaluated in $\phi_{1,0}$ and $\phi_{2,0}$. In Eq. (6), the zero-order contribution that does not depend on the PSs intrinsic fluctuations, and represents the quantum photon noise of the measurement, while the statistical characteristics of the phase noise enter as second-order contributions.

Here we focus on the problem of reducing the photon noise below the shot noise in the measurement of phase covariance. Of course, this means to look for the HN in a region of the noise spectrum that is shot-noise limited where all the sources of technical noise, like mechanical and acoustic vibration, thermal noise and others are suppressed. This is possible because HN is expected to have a characteristic bandwidth which extends up to $c/2L$, where c is the speed of the light and L is the arms length. For L of the order of one meter it reaches tens of MHz. Therefore, the zero-order uncertainty that we will study here is

$$\mathcal{U}^{(0)} = \frac{\sqrt{2 \text{Var} [\hat{C}(\phi_{1,0}, \phi_{2,0})]}}{|\langle \partial_{\phi_1, \phi_2}^2 \hat{C}(\phi_{1,0}, \phi_{2,0}) \rangle|}. \quad (7)$$

In the following we consider two possible quantum states feeding the free input ports of \mathcal{I}_k and two related readout strategies.

3.1 Readout strategy 1: two squeezed states

The state of two uncorrelated single-mode squeezed states writes:

$$|\xi\rangle_{a_1} \otimes |\xi\rangle_{a_2} = S_{a_1}(\xi) S_{a_2}(\xi) |0\rangle_{a_1} \otimes |0\rangle_{a_2}$$

where $S_{a_k}(\xi) = \exp[\frac{1}{2}\xi (a_k^\dagger)^2 - \frac{1}{2}\xi^* (a_k)^2]$ is the squeezing operator. If we set $\xi = |\xi|e^{i\theta_\xi}$, then $\lambda = \sinh^2 |\xi|$ represents the average number of photons of the squeezed vacuum, taken equal in both the modes.

Defining the the quadrature of the field as:

$$x_k = \frac{a_k + a_k^\dagger}{\sqrt{2}} \quad \text{and} \quad y_k = \frac{a_k - a_k^\dagger}{i\sqrt{2}},$$

and supposing y_k the squeezed and x_k the anti-squeezed one, i.e., $\xi_k = |\xi_k| \geq 0$, it is known that the output port of a single interferometer with strong coherent beam in one input, is proportional to the quadrature of the field at the other input port. Thus, the injection of a squeezed state provides a fixed factor $\langle \delta y_k^2 \rangle = e^{-2\xi_k}$ of resolution enhancement, which corresponds to the variance of the squeezed quadrature.¹¹

We expected that the increased resolution in the estimation of the phase shifts ϕ_1 and ϕ_2 separately reflects in a better estimation of their correlation if the correlation of the squeezed quadratures of the output modes c_k are considered. It is rather intuitive that the most simple form of the measurement operator $\hat{C}(\phi_1, \phi_2)$, that combines the squeezed quadratures measured at the read-out port, and has non-null mixed derivative with respect to the phases, $\partial_{\phi_1, \phi_2}^2 \hat{C} \neq 0$, would be the product $Y_1 Y_2$ (where Y_k are the squeezed quadratures). However, to avoid the presence of a dc-component in the measurement it turns out more useful to consider the fluctuation of the quadratures around their central value, therefore defining $\hat{C} = \{Y_1(\phi_1) - \mathcal{E}[Y_1]\} \{Y_2(\phi_2) - \mathcal{E}[Y_2]\}$, where we have taken into account that $\mathcal{E}_\parallel[Y_k] = \mathcal{E}_\perp[Y_k] = \mathcal{E}[Y_k]$. The covariance of the phases is estimated according to Eq. (4) as:

$$\mathcal{E}_\parallel [\delta\phi_1 \delta\phi_2] \approx \frac{\mathcal{E}_\parallel [Y_1 Y_2] - \mathcal{E}_\perp [Y_1 Y_2]}{\langle \partial_{\phi_1, \phi_2}^2 Y_1(\phi_0) Y_2(\phi_0) \rangle}. \quad (8)$$

Since the fluctuations of the quadratures due to quantum noise are independent in the two interferometers, the zero-order uncertainty on the measured observable remains $\text{Var}[\hat{C}(\phi_{1,0}, \phi_{2,0})] = \langle \{Y_1(\phi_0) - \mathcal{E}[Y_1]\}^2 \rangle \langle \{Y_2(\phi_0) - \mathcal{E}[Y_2]\}^2 \rangle$ [see Eq. (7)].

3.2 Readout strategy 2: TWB

The TWB correlated state can be expressed in the Fock bases $\{|m\rangle_{a_k}\}$ as

$$|\Psi(\lambda)\rangle_{a_1,a_2} = \frac{1}{\sqrt{1+\lambda}} \sum_{m=0}^{\infty} \left(e^{i\theta} \sqrt{\frac{\lambda}{1+\lambda}} \right)^m |m, m\rangle_{a_1,a_2} \quad (9)$$

where $|m, m\rangle_{a_1,a_2} = |m\rangle_{a_1} \otimes |m\rangle_{a_2}$ and θ is the phase, which we set in the following to $\theta = 0$ without loss of generality. The TWB presents perfect correlations in the photon number $m_k \equiv a_k^\dagger a_k$ meaning that $_{a_1,a_2} \langle \Psi(\lambda) | (m_1 - m_2)^M | \Psi(\lambda) \rangle_{a_1,a_2} = 0$, $\forall M > 0$ integer. It suggests to choose the measurement operator in the same form $\hat{C}(\phi_1, \phi_2) = (N_1 - N_2)^M$, $M > 0$, since this should correspond to a reduction of the photon noise in the measurement, finally improving the sensitivity. We notice immediately that for $M = 1$, corresponding to the photon numbers difference, the proportional coefficient in Eq. (4), containing the double derivative with respect to both the phases will be null. Thus, we have to move to the second order measurement, i.e. $\hat{C}(\phi_1, \phi_2) = [N_1(\phi_1) - N_2(\phi_2)]^2 = N_1^2 + N_2^2 - 2N_1N_2$. Hereinafter we also consider the same central phase of the two interferometers $\phi_{1,0} = \phi_{2,0} = \phi_0$.

According to Eq. (4) we get:

$$\mathcal{E}_{||} [\delta\phi_1 \delta\phi_2] \approx \frac{\mathcal{E}_{||} [N_1 N_2] - \mathcal{E}_{\perp} [N_1 N_2]}{\langle \partial_{\phi_1, \phi_2}^2 N_1(\phi_0) N_2(\phi_0) \rangle}, \quad (10)$$

where we have used again the symmetry of the statistical properties of the two interferometers, in particular $\mathcal{E}_{||(\perp)} [N_1^2] = \mathcal{E}_{\perp(||)} [N_2^2]$. The covariance of the phase noise is proportional to the difference between the photon number correlation when the phase noise is correlated ($||$) and when it is not (\perp), as one could expect.

The uncertainty of the measurement, due to photon noise can be obtained by Eq. (7) where $\text{Var}[\hat{C}(\phi_{1,0}, \phi_{2,0})] = \langle [N_1(\phi_0) - N_2(\phi_0)]^4 \rangle - \langle [N_1(\phi_0) - N_2(\phi_0)]^2 \rangle^2$.

4. RESULTS

The analytical calculation of the variance of the measurement operator $\hat{C}(\phi_0)$, in particular for TWB case, involves many fourth-order terms of the photon number operator, i.e. eighth-order product of field operator c_k and c_k^\dagger , and the calculation and the complete expression of this variance are too cumbersome to be reported here. Thus, we will present numerical results for the most significant regions inside the parameter space and we give some general expression in particular relevant limits. First of all we need to define the classical benchmark to compare performance using quantum light. The uncertainty achievable in the estimation of the phase covariance, if only the coherent beams are used, is $\mathcal{U}_{\text{CL}}^{(0)} = \sqrt{2}/(\eta\mu \cos^2[\phi_0/2])$. It is worth noting that it scales as the detected number of photons, i.e., the *square* of the shot noise limit typical of the single phase estimation. This directly follows from the measurement of a second order quantity, namely the covariance of the phases.⁹ As usual, it is clear that without any particularly energy constraint, in order to reach high sensitivity in a phase-correlation measurement it is necessary to push the intensity of the classical field. Therefore, even the quantum strategy should face and improve the sensitivity when high power is circulating into the interferometers. Therefore, we will consider the limit $\mu \gg 1$.

Concerning the use of the two independent squeezed states, we can summarize the results in the following two equations for the ratio $\mathcal{R}_{\text{SQ}}^{(0)} = \mathcal{U}_{\text{SQ}}^{(0)}/\mathcal{U}_{\text{CL}}^{(0)}$ in the limit $\mu \gg 1$:

$$\mathcal{R}_{\text{SQ}}^{(0)} \approx 1 - \frac{\eta(1 + \cos \phi_0)}{2} + \frac{\eta \cos^2(\phi_0/2)}{4\lambda} \quad (\lambda \gg 1), \quad (11a)$$

$$\mathcal{R}_{\text{SQ}}^{(0)} \approx 1 - \eta(1 + \cos \phi_0)\sqrt{\lambda}(1 - \sqrt{\lambda}) \quad (\lambda \ll 1). \quad (11b)$$

As a matter of fact, we expect that the advantages of using squeezing, and in general quantum light, is effective in the presence of a low loss level. Thus the most interesting regime is when the two interferometers transmit almost all the quantum light to the read-out port. In this case the central phase must be close to 0,

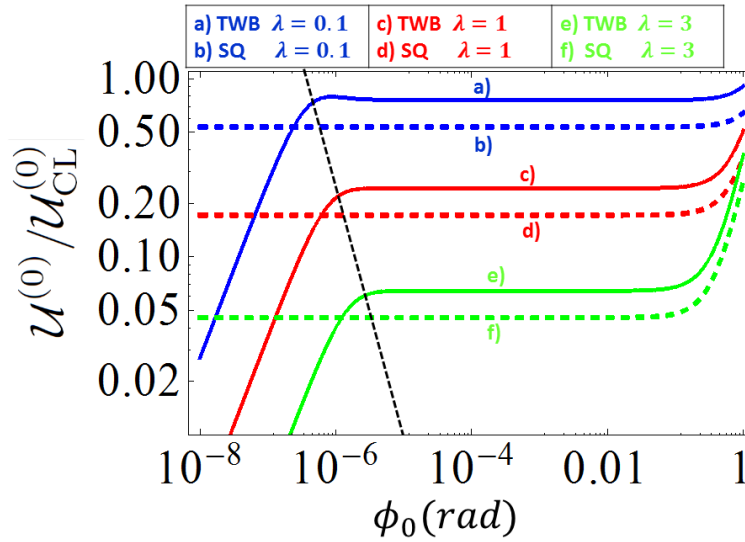


Figure 2. (Color online) Log-log-plot of the quantum enhancements provided by the TWB (solid lines) and by the squeezing (dashed lines) as a function of the central phase ϕ_0 for three different values of the mean number of photons per mode λ of the quantum light. We set $\eta = 1$, $\mu = 3 \times 10^{12}$, $\psi = \pi/2$.

according to the BS-like behaviour $\tau = \cos^2(\phi_0/2) \simeq 1$. In this limit Eqs. (11) reduce to $\mathcal{R}_{\text{SQ}}^{(0)} \approx 1 - \eta + \eta/4\lambda$ for $\lambda \gg 1$ and $\mathcal{R}_{\text{SQ}}^{(0)} \approx 1 - 2\eta\sqrt{\lambda}(1 - \sqrt{\lambda})$ for $\lambda \ll 1$. Fig. 2 reports the exact uncertainty reduction in function of the central phase ϕ_0 for the ideal lossless case. As expected, the uncertainty lower bound is determined by the value of the squeezing parameter, in other terms by the mean photon number of the squeezed beam λ . The dependence on the detection efficiency η is shown in Fig. 3.

Concerning TWB, one can clearly discern two completely different scaling of the uncertainty in Fig. 2 which corresponds to two different type of correlation at the read-out ports generated by the action of the interferometers on the TWB state.

Photon number entanglement

If intensity at the read-out port is dominated by the TWB, namely the condition $\mu(1 - \tau)/\tau\lambda \ll 1$ is fulfilled, the perfect photon number correlation are preserved, since the coherent beam is completely addressed to the other output port (not detected). In this case the initial entanglement of the TWB state allows making the uncertainty on the observable $\hat{C}(\phi_1, \phi_2) = [N_1(\phi_1) - N_2(\phi_2)]^2$ arbitrary small. The condition is guaranteed if the central phases are close enough to zero, namely, $\phi_{1,0} = \phi_{2,0} \simeq 0$, meaning that the interferometers transmission τ approaches the unity. Anyway it appears quite challenging to achieve in the cases of practical interest in which the coherent mode is largely populated: the larger is μ , the closer to unity has to be the interferometer transmission τ . This is the regime studied and reported in.⁹ For intense coherent beam and intense TWB source, i.e. $\mu \gg \lambda \gg 1$, one gets $\mathcal{R}_{\text{TWB}}^{(0)} = \mathcal{U}_{\text{TWB}}^{(0)}/\mathcal{U}_{\text{CL}}^{(0)} \approx 2\sqrt{5}(1 - \eta)$, while in the case of faint TWB, $\lambda \ll 1$ and $\mu \gg 1$, the result is $\mathcal{R}_{\text{TWB}}^{(0)} \approx \sqrt{2(1 - \eta)}/\eta$. In both cases TWB allows reaching a dramatic uncertainty reduction that approaches zero for $\eta \rightarrow 1$. This behaviour is clearly shown in Fig. 3: the choice of μ and ϕ_0 ensures to be in the TWB-like regime (at least for the considered range of values of λ). The ratio $\mathcal{R}_{\text{TWB}}^{(0)}$ always drop to zero as $\eta \rightarrow 1$, whereas for η larger than a threshold value η_{th} we have $\mathcal{R}_{\text{TWB}}^{(0)} < \mathcal{R}_{\text{SQ}}^{(0)}$. We have also reported the limits for $\lambda \ll 1$ and for $\lambda \gg 1$. Overall, we observe that for quantum light intensity $\lambda > 1$ reachable in experiments nowadays (for example $\lambda = 3$ in the picture) squeezing performs better than TWB except for demanding overall detection efficiency.

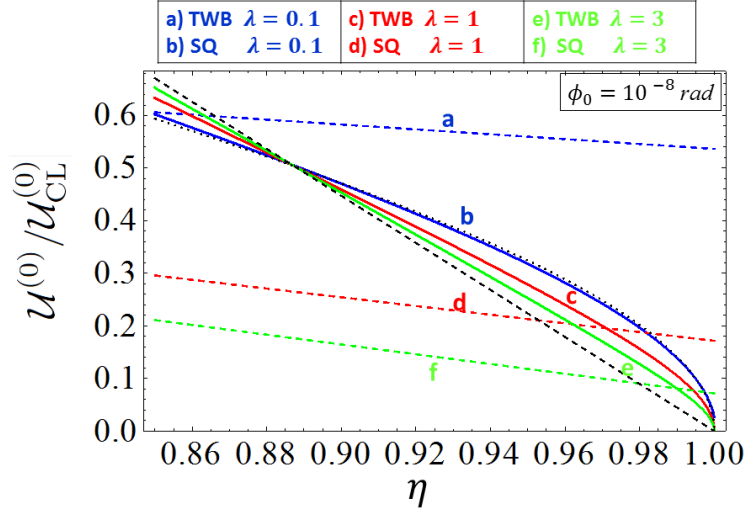


Figure 3. (Color online) Plot of the quantum enhancements provided by the TWB (solid lines) and by squeezing (dashed lines) as a function of the quantum efficiency η for different values of the mean number of photons per mode λ of the quantum light. We set $\phi_0 = 10^{-8} \text{ rad}$, $\mu = 3 \times 10^{12}$, $\psi = \pi/2$. We also reported the limits for $\lambda \ll 1$ (black-dotted line) and for $\lambda \gg 1$ (black-dashed line) referring to the TWB.

Moreover, in order to demonstrate that entanglement has a fundamental role in the strong uncertainty reduction, in other words to show that the phase coherence of the TWB state is necessary, we now consider a Gaussian phase noise of the form $\frac{e^{-\frac{\theta^2}{2\sigma^2}}}{\sqrt{2\pi\sigma^2}}$ acting on the phase θ of the TWB state in Eq. (9). Therefore the initial state $\rho_{TWB} = |\Psi(\lambda)\rangle\langle\Psi(\lambda)|$ in input becomes a mixed state expressed by

$$\rho_{mix}(\sigma) = \int \delta\theta \rho_{TWB} \frac{e^{-\frac{\theta^2}{2\sigma^2}}}{\sqrt{2\pi\sigma^2}}$$

The density matrix of the state after decoherence, expressed in the base of the photon numbers is

$$\rho_{mix}^{(n,m)}(\sigma) = \sum_{n,m} (1 - \lambda^2) \lambda^{m+n} e^{-\frac{1}{2}\sigma^2(m-n)^2} |n, n\rangle\langle m, m| \quad (12)$$

When the noise distribution is Dirac function, for $\sigma \rightarrow 0$, one retrieves the form of the TWB state, while if strong dephasing take place, for $\sigma \gg 1$, the state becomes diagonal (only the terms with $n = m$ survive), nonetheless maintaining perfect non-classical correlation of the photon number. The degree of entanglement of the state can be evaluated by the negativity calculated according to the prescription of Ref.¹² and is reported in Fig. 4a for three different values of the mean number of photon per mode. On the other side it is expected that the phase coherence in the interferometer is essential. Actually, the sensitivity coefficient appearing at the denominator of Eq.s (7) and (4) depends on the relative phase difference between the TWB and the coherent input. Setting for simplicity the working phases exactly to $\phi_{1,0} = \phi_{2,0} \simeq 0$, one gets:

$$\langle \partial_{\phi_1, \phi_2}^2 N_1(\phi_0) N_2(\phi_0) \rangle = \frac{1}{2} \mu \eta^2 \sqrt{\lambda(\lambda+1)} \cos[2(\psi - \theta)] \quad (13)$$

It is clear that random phase fluctuation will deteriorate the sensitivity coefficient. The effect of the action of the Gaussian noise on the coefficient calculated as $\int \delta\theta \langle \partial_{\phi_1, \phi_2}^2 N_1(\phi_0) N_2(\phi_0) \rangle \frac{e^{-\frac{\theta^2}{2\sigma^2}}}{\sqrt{2\pi\sigma^2}}$ is reported in Fig. 4b. We note that the sensitivity coefficient drops to zero in the same way as the negativity of the state at the increasing of the dephasing noise. This demonstrate the role of the entanglement in the double interferometer scheme.

Non-classical correlations

In the opposite case, i.e. $\mu(1-\tau)/\tau\lambda \gg 1$ for intermediate values of the central phase ϕ_0 , the uncertainty reduction for $\mu \gg 1$ behaves as for the two independent squeezing case (aside a constant factor $\sqrt{2}$). Specifically, $\mathcal{R}_{\text{TWB}}^{(0)} = \sqrt{2} \mathcal{R}_{\text{SQ}}^{(0)}$. It can be easily appreciated when comparing the corresponding curves for $\mathcal{R}_{\text{TWB}}^{(0)}$ and $\mathcal{R}_{\text{SQ}}^{(0)}$ in Fig. 2 (note the logarithmic scale).

This can be understood by considering that the single interferometer performs a measurement of the quadrature of the single TWB mode $x_k(y_k)$. In particular, in our system, the measurement of $[N_1(\phi_1) - N_2(\phi_2)]^2$ closely correspond to the measurement of $\langle \delta(x_1 - x_2)^2 \rangle$ of the TWB, which is known to be indeed squeezed in the form $\langle \delta(x_1 - x_2)^2 \rangle = e^{-2|\xi|}/2$. In fact, this is the same improvement obtained by the double squeezed state.

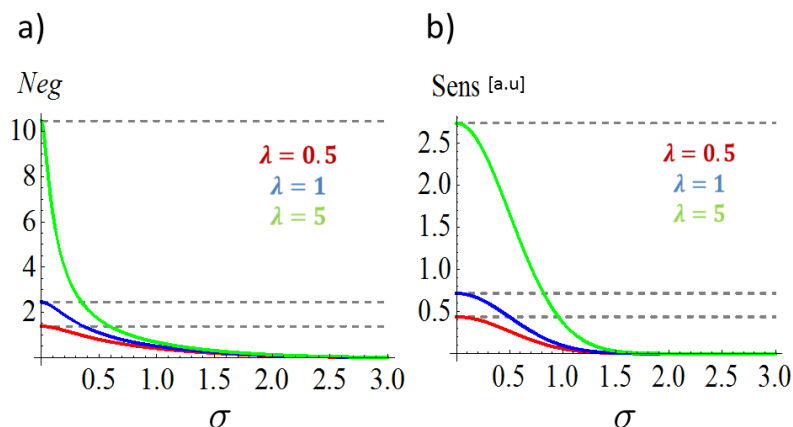


Figure 4. Entanglement role in the sensitivity: transition from the photon number entangled state to an incoherent mixed state for three different values of the mean photon number per mode λ are considered. a) Negativity of the state in function of the amplitude of the Gaussian distribution of the phase noise (see text for details). b) Sensitivity coefficient in the measurement of the phase covariance in function of the amplitude of the Gaussian distribution of the phase noise. The curves are reported in arbitrary units because they are normalized by the constant factor $\mu\eta^2$.

5. CONCLUSION

We have studied in detail a system of two interferometers aimed at detecting extremely faint phase-fluctuations. This system can represent a breakthrough for detecting a faint correlated signal that would remain otherwise undetectable even using the most sensitive individual interferometric devices, as in the case of the so-called “holographic noise”. The signature of this kind of noise emerges as a correlation between the output signals of the interferometers. We show how injecting quantum light in the free ports of the interferometers can reduce the photon noise of the system beyond the shot-noise, enhancing the resolution in the phase-correlation estimation. We analyze both the use of two-mode squeezed vacuum and of two independent squeezed states. On the one hand, our results confirm the benefit of using squeezed beams together with strong coherent beams in interferometry. On the other hand we investigate the possible use of two-mode squeezed vacuum, discovering interesting and unexplored areas of application of bipartite entanglement and in particular the possibility of reaching in principle surprising uncertainty reduction.

5.1 Acknowledgments

This publication was made possible through the support of the John Templeton Foundation (Grant ID 43467). The opinions expressed in this publication are those of the authors and do not necessarily reflect the views of the John Templeton Foundation.

REFERENCES

- [1] G. Amelino Camelia, Nature **398**, 216 (1999).
- [2] G. Amelino Camelia, Nature **478**, 466 (2011).
- [3] I. Pikovski, M. R. Vanner, M. Aspelmeyer, M. S. Kim and Časlav Brukner, Nat. Phys. **8**, 393 (2012).
- [4] J. D. Bekenstein, arXiv:1211.3816 (2012).
- [5] G. Hogan, Phys. Rev. D **85**, 064007 (2012).
- [6] P. Aschieri, and L. Castellani, Journ. of Geom. and Phys. **60**, 375 (2010).
- [7] Aaron S. Chou *et al*, arXiv:1512.01216
- [8] J. Abadie, *et al.*, Nature Phys **7**, 962 (2011).
- [9] I. Ruo Berchera, I. P. Degiovanni, S. Olivares, M. Genovese Phys. Rev. Lett. **110**, 213601 (2013).
- [10] I. Ruo-Berchera, I. P. Degiovanni, S. Olivares, N. Samantaray, P. Traina, and M. Genovese, Phys. Rev. A **92**, 053821 (2015).
- [11] C. M. Caves, Phys. Rev. D **23** , 1693 (1981).
- [12] M. Roncaglia, A. Montorsi, M. Genovese, Phys. Rev A **90**, 062303 (2014).